

On the fabrication of high-surface-area and high-aspect-ratio gold nanostructures

Marco Riccardi¹

¹*Nanophotonics and Metrology Laboratory, Swiss Federal Institute of Technology Lausanne (EPFL), EPFL-STI-NAM, Station 11, CH- 1015 Lausanne, Switzerland*

We highlight some stability issues in high-surface-area and high-aspect ratio gold nanostructures fabricated using inorganic adhesion layers on silica substrates. We ascribe these problems to capillary and surface effects and show the use of organic silane self-assembled monolayers to improve the long-term stability of such structures.

Keywords: gold; aspect ratio; surface area; stability; adhesion layer; self-assembled monolayer

The fabrication of high-aspect-ratio nanostructures is notoriously difficult due to the high asymmetry of these systems. We describe here a way to fabricate arrays of interdigitated nanoelectrodes having extremely high aspect ratios such as the ones shown in Figure 1. Each electrode here, circled in red, is $25\text{ }\mu\text{m}$ long and between 70 and 150 nm wide, resulting in an aspect ratio greater than 200; while the total structure has got a surface area of about $10^4\text{ }\mu\text{m}^2$ and a specific surface area greater than $1\text{ m}^2/\text{g}$. At the end of each electrode, a cylinder is also fabricated for plasmonic applications (see Figure 2 on the right). The structures, which are 40 nm high, are made of polycrystalline gold and are fabricated using e-beam lithography on a double-layer MMA/PMMA positive resist coated on a glass wafer. Figure 2 shows the structures straight after the fabrication process, where a 3 nm Ti adhesion layer was used

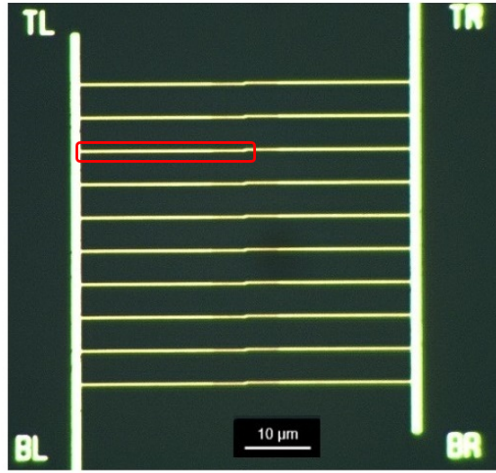


FIG. 1: Dark-field optical image of an array of interdigitated electrodes.

to promote the adhesion of gold onto the silica substrate and a 8 s O_2 descum (300 sccm, 2 Torr, 500 W RF power) was performed before the metal evaporation to remove the residuals of undeveloped resist and chemically activate the surface. We see that we are able to nicely fabricate all the electrodes, with a fabrication yield close to 100%. However, a few hours later the structures are all destroyed, as shown in Figure 3. In particular we see here on the right that the gold has escaped the predefined pattern written in the resist and has reorganized into spherical shapes. We attribute this behaviour to surface forces which govern the behaviour of the gold arranged in this high-surface-area geometry [1] and force it to transition to a more stable spherical shape with reduced surface area. To counteract this effect and stabilize the whole geometry, we tried different adhesion layers in the hope to better anchor the gold to the substrate. In particular, we tested a Cr adhesion layer, which helped improving the fabrication results thanks to the higher diffusion of Cr atoms into the gold layer [2]. Indeed we see in Figure 4 on the right that a 10 nm Cr adhesion layer is able to fully stabilize the structures, which are now able to survive multiple weeks outside the cleanroom.

Unfortunately, it is known that thick adhesion layers can be detrimental for some applications [3, 4]. In particular, the use of a 10 nm Cr layer to stabilize 40 nm-tall gold nanostructures is to be avoided in order, for example, to prevent a deterioration of the optical properties of the structures. We therefore developed a process to use a thin organic self-assembled monolayer (SAM) as an adhesion layer between the silica substrate and the gold structures. We chose to work with (3-Mercaptopropyl)trimethoxysilane (MPTMS, from Merck), a silane molecule having a thiol group (SH) at one end and methoxy groups (O-CH_3) at the other as shown in Figure 5.

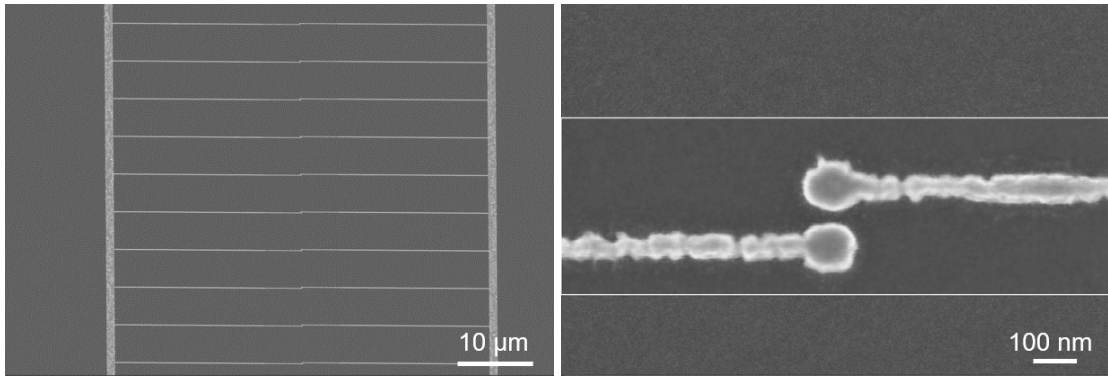


FIG. 2: SEM images of the structures straight after the fabrication. A 1.5 nm Cr layer is sputtered on top to avoid charging issues during imaging.

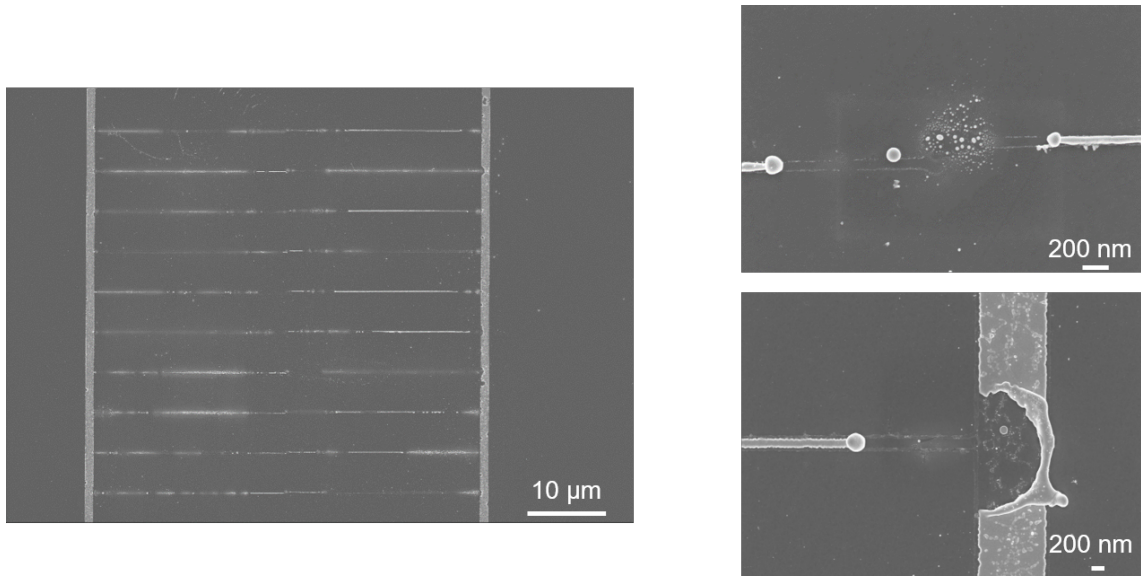


FIG. 3: SEM images of the fabricated structures using a 3 nm Ti adhesion layer a few hours after the end of the fabrication process. The sample is kept in normal cleanroom ISO5 atmosphere. A 1.5 nm Cr layer is sputtered on top to avoid charging issues during imaging.

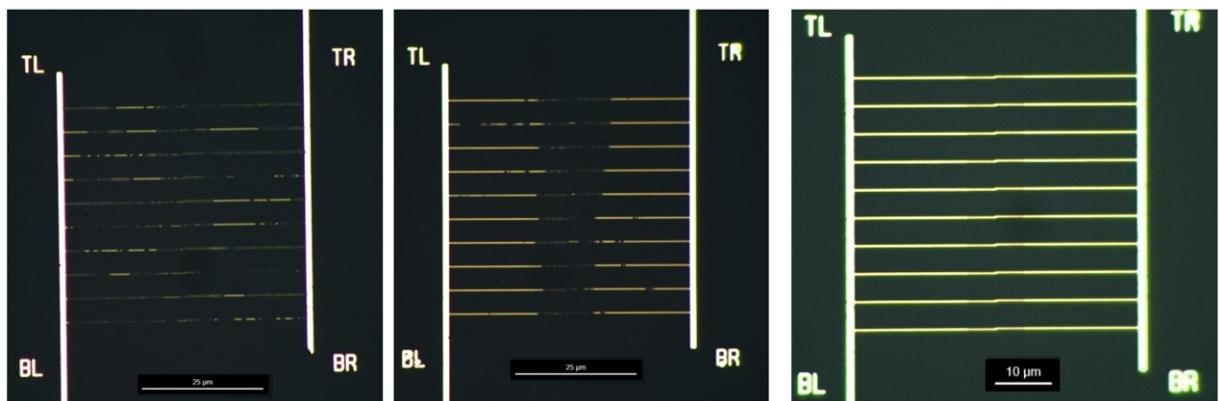


FIG. 4: Optical dark-field images of the structures several weeks after their fabrication. The structures are fabricated with a 3 nm Ti adhesion layer (left), a 3 nm Cr adhesion layer (middle) and a 10 nm Cr adhesion layer (right).

The sulphur atom in the thiol group forms a strong covalent bond with gold [5, 6], while the methoxy groups are known to hydrolyse in the presence of water and form siloxane (Si-O-Si) bridges with a chemically-active silica substrate [7, 8]. This way, MPTMS can act as a molecular linker between the gold and the glass substrate, connecting them through a series of covalent bonds that provide a stronger binding force than the one between Ti or Cr and gold. In order to form an ordered SAM on the silica surface, we first chemically activate this substrate using an O₂ plasma treatment (40 s, 300 sccm, 2 Torr, 500 W RF power) to create hydroxy groups (OH) on its surface. The MPTMS molecules are then evaporated on the substrate [9] for about 10 hours before the substrate is baked at 80°C for roughly 24 hours to promote the reaction between the MPTMS molecules and the OH groups on the glass. At the end of this process, the substrate now presents at its surface a layer of thiol groups which can readily bind to gold, once this is evaporated on the sample. After the metal evaporation, an additional baking step (24 hours at 80°C) is also performed to further stabilize the gold nanostructures. The fabrication steps of the SAM are depicted in Figure 6, while Table I provides a detailed fabrication process of the whole structure. Figure 7 shows some SEM images of the fabricated sample several

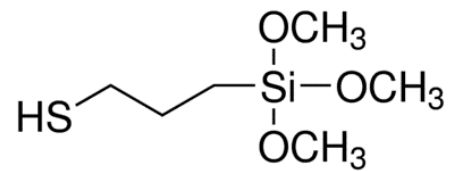


FIG. 5: MPTMS molecule (from the Merck website).

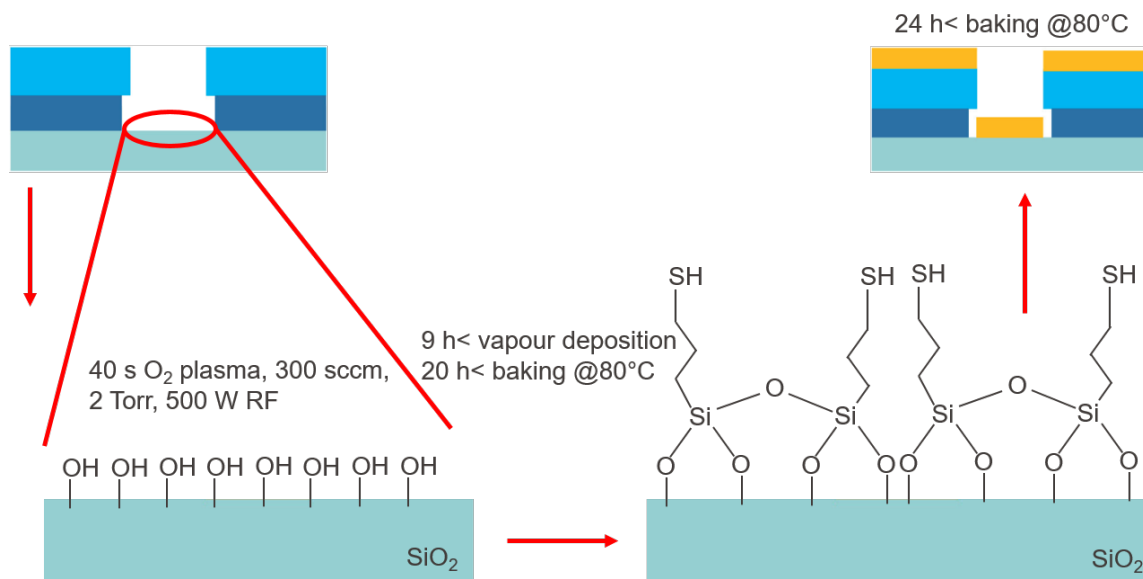


FIG. 6: Creation of a MPTMS adhesion layer for gold on a silica substrate. More details are provided in Table I.

weeks after the lift-off. Clearly, the organic adhesion layer is able to improve the long term stability of the structures as these are still all in place on the substrate, as opposed to the ones fabricated with the standard inorganic adhesion layers shown in figure 3 and 4. Organic SAMs therefore provide a better way to anchor gold nanostructures to silica substrate and are particularly helpful when working with high-surface-area and high-aspect-ratio geometries.

After showing the benefits of using SAMs as adhesion layers we also provide, for completeness, a list of possible issues and complications that might arise during this kind of process:

1. Generally, as shown in Figure 8, some residuals of resist which had not lifted off were often found around the structures, especially those written with higher e-beam doses. Sonicating the sample in acetone for a few minutes helped removing the unwanted resist, but was also found to damage these delicate structures. Likewise, long SAM evaporation times (greater than 12 hours) were also found to make the lift-off more challenging. To this end, the relatively long O₂ treatment used to activate the silica surface also inherently etches the resist, which can become an issue as different resist flakes can be bridged together while the resist melts during the plasma, making the lift-off more challenging. To avoid this problem, additional apertures can be created in the resist during the e-beam exposure.
2. As shown in Figure 9 it is challenging, with this process, to fabricate structures smaller than about 80 nm, as the final structures can be several times larger than the pattern written in the resist. In particular, the e-beam

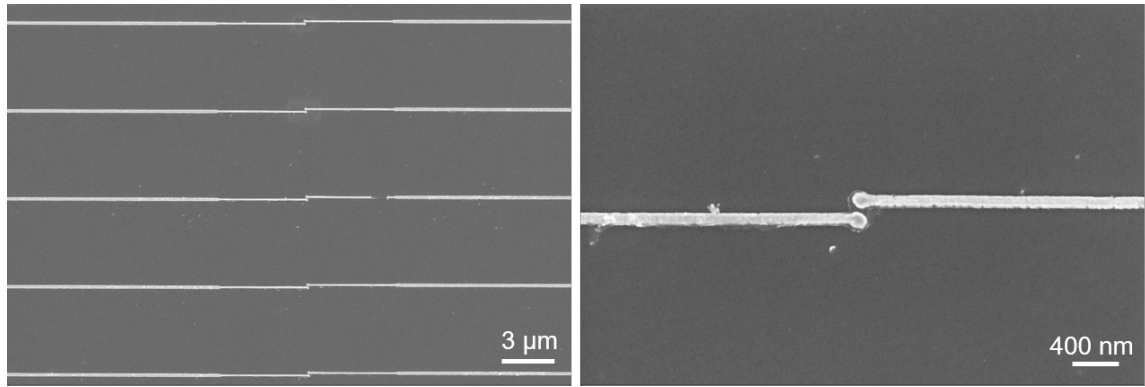


FIG. 7: SEM images of the fabricated structures using a MPTMS adhesion layer several weeks after the lift-off. The sample is kept in normal cleanroom ISO5 atmosphere. A 1.5 nm Cr layer is sputtered on top to avoid charging issues during imaging.

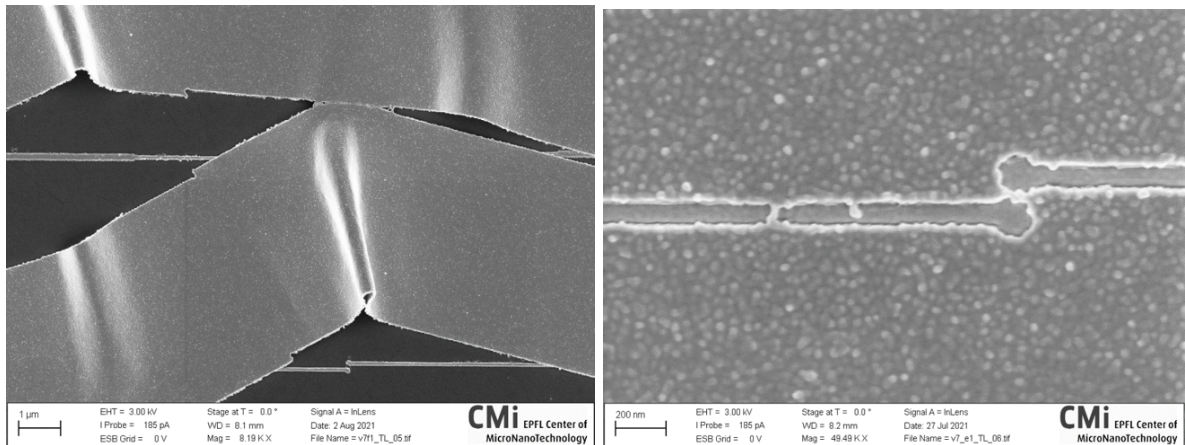


FIG. 8: SEM images of different samples after lift-off. Some flakes have been bridges together and have not been removed from the substrate.

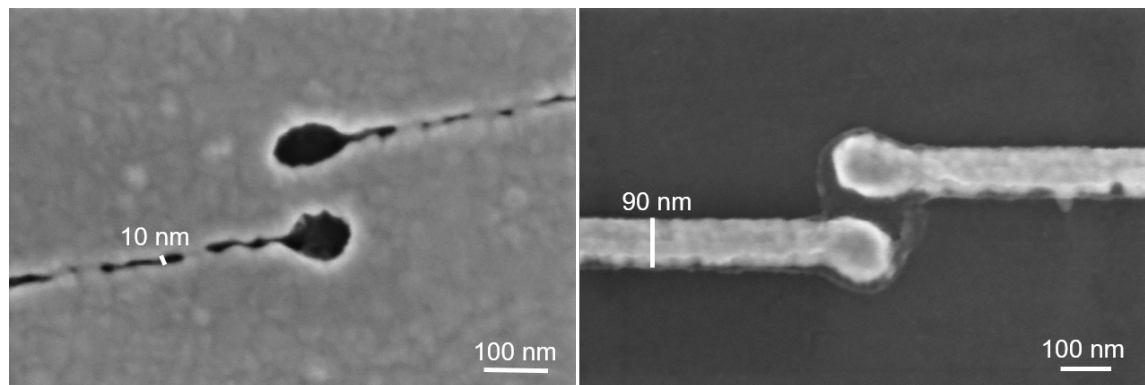


FIG. 9: Left: SEM image of the PMMA mask from a remaining flake of resist left on the substrate after the lift-off. Right: SEM image of the fabricated electrodes. A 1.5 nm Cr layer is sputtered on top to avoid charging issues during imaging.

dose has to be reduced to up to ten times less than the one used with inorganic adhesion layers. This is due to the fact that the diffusion of gold is enhanced over the goldphilic thiolated silica surface and gold adatoms can therefore greatly diffuse underneath the resist undercut during the metal deposition. To this end, since PMMA is less soluble than MMA in the developer solution and therefore generates smaller undercuts, its use as the bottom layer resist might help shrinking the final size of the structures.

3. Preliminary tests have also been performed with an alternative fabrication process employing HSQ. Briefly, the HSQ is coated on a silica-MPTMS-Au-Cr substrate and used as a mask for the ion-beam etching (IBE) of the unwanted metal, followed by wet etching of the sacrificial Cr layer. In principle, this approach is able to solve both the issues mentioned above, but carries its own problems. In particular, the MPTMS SAM can be damaged by the acidic Cr etch solution and, moreover, great care must be taken during the IBE as to not charge the two electrodes in the final part of the process, leading to electrostatic repulsion and explosion (see Figure 10).

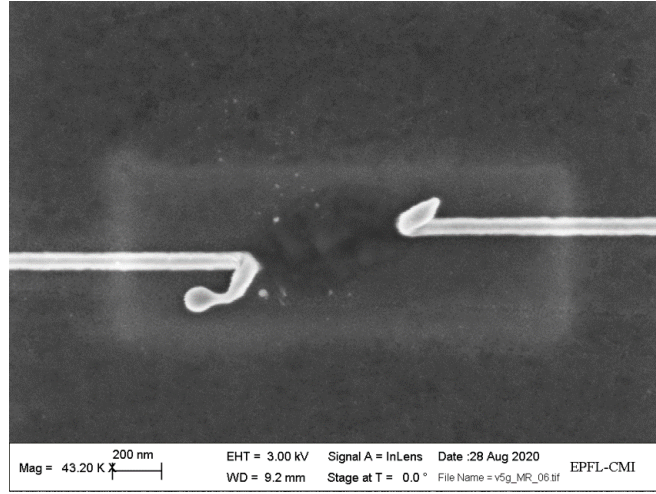








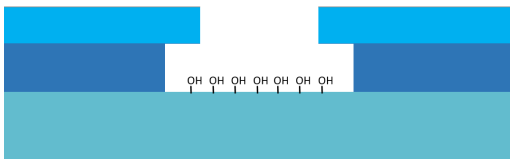
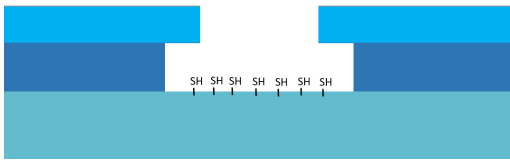
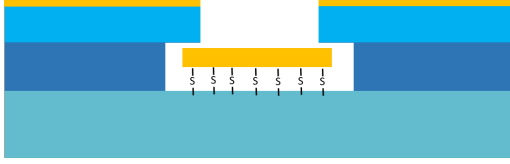
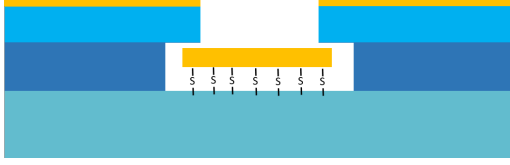


FIG. 10: SEM image of a pair of exploded electrodes due to electrostatic repulsion during IBE. These structures were fabricated with an inorganic Ti adhesion layer. A 1.5 nm Cr layer is sputtered on top to avoid charging issues during imaging.

We conclude by providing a detailed step-by-step fabrication process:

0: Substrate	
4-inch fused silica wafer (100% SiO ₂), 525 μ m thick	
1: Substrate dehydration	
5 min at 180°C	
2: Bottom resist layer spincoating	
120 nm of MMA EL6, 6000 rpm + 5 min at 180°C	
3: Top resist layer spincoating	
60 nm of PMMA 495K A2, 1500 rpm + 5 min at 180°C	

<p>4: Conductive layer deposition</p> <p>E-beam evaporation of 20 nm of Cr</p>	
<p>5: E-beam exposure</p> <p>E-beam dose between 500 and 2000 $\mu\text{C}/\text{cm}^2$</p>	
<p>6: Conductive layer etching</p> <p>Cr wet etching in a $(\text{NH}_4)_2\text{Ce}(\text{NO}_3)_6 + \text{HClO}_4$ solution</p>	
<p>7: Development</p> <p>1 min in MiBK:IPA 1:3 + 1 min rinse in IPA</p>	
<p>8: Surface activation</p> <p>O_2 plasma, 40 s, 300 sccm, 2 Torr, 500 W RF power</p>	
<p>9: SAM assembly</p> <p>10 h MPTMS evaporation + 20 h at 80°C</p>	
<p>10: Metal evaporation</p> <p>E-beam evaporation of 40 nm of Au, 0.5 $\text{\AA}/\text{s}$</p>	
<p>11: Stabilization bake</p> <p>24 h at 80°C</p>	
<p>12: Lift-off</p>	

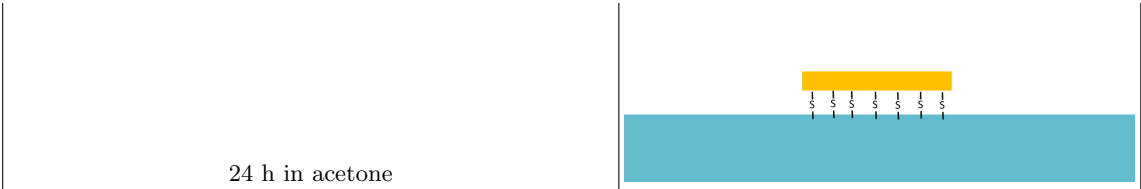


TABLE I: Process flow of the fabrication process.

-
- [1] N. Mameka, J. Markmann, and J. Weissmüller, *Nature Communications* **8**, 1976 (2017), URL www.nature.com/naturecommunications.
 - [2] M. Todeschini, A. Bastos da Silva Fanta, F. Jensen, J. B. Wagner, and A. Han, *ACS Applied Materials & Interfaces* **9**, 37374 (2017), URL www.acsami.org.
 - [3] D. Barchiesi, D. Macías, L. Belmar-Letellier, D. Van Labeke, M. Lamy De La Chapelle, T. Toury, E. Kremer, L. Moreau, and T. Grosge, *Applied Physics B* **93**, 177 (2008).
 - [4] M. Najiminaini, F. Vasefi, B. Kaminska, and J. J. Carson, *Optics Express* **19**, 26186 (2011).
 - [5] C. Vericat, M. E. Vela, G. Benitez, P. Carro, and R. C. Salvarezza, *Chemical Society Reviews* **39**, 1805 (2010), URL www.rsc.org/csr.
 - [6] H. Häkkinen, *Nature Chemistry* **4** (2012), URL www.nature.com/naturechemistry.
 - [7] C. M. Halliwell and A. E. G. Cass, *Analytical Chemistry* **73**, 2476 (2001), URL <https://pubs.acs.org/sharingguidelines>.
 - [8] G. J. Zhang, T. Tani, T. Zako, T. Hosaka, T. Miyake, Y. Kanari, T. Funatsu, and I. Ohdomari, *Small* **1**, 833 (2005).
 - [9] N. R. Glass, R. Tjeung, P. Chan, L. Y. Yeo, and J. R. Friend, *Biomicrofluidics* **5**, 036501 (2011), URL <https://doi.org/10.1063/1.3625605>.